#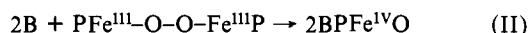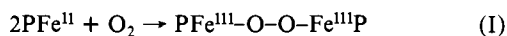 Nuclear Magnetic Resonance Studies of Axial Amine Coordination in Synthetic Ferryl, $(Fe^{IV}O)^{2+}$, Porphyrin Complexes and in Ferryl Myoglobin

Alan L. Balch,* Gerd N. La Mar,* Lechoslaw Latos-Grazynski, Mark W. Renner, and V. Thanabal

Contribution from the Department of Chemistry, University of California, Davis, California 95616. Received October 22, 1984

Abstract: Proton and deuterium NMR studies have detected resonances of coordinated pyridine, 1-methylimidazole, and their derivatives in synthetic ferryl, $(Fe^{IV}O)^{2+}$, porphyrin complexes. The resonances have been identified through methyl and deuterium labeling. Only one amine ligand is present and it must exchange slowly with the free ligand. The results for these synthetic model complexes have led to the detection of broad, weak axial histidine resonances at -11 and -16 ppm in ferryl myoglobin at 35 °C. Analysis of the hyperfine shifts in these paramagnetic molecules suggests that the axial amine is located trans to a strongly π-donating oxo ligand in both the model compounds and ferryl myoglobin.

Iron porphyrin complexes containing the ferryl unit, $(Fe^{IV}O)^{2+}$, are available synthetically via the two step sequence shown in eq I and II[1-5] where P is a porphyrin dianion and B can be pyridine (py), 1-methylimidazole (1-CH$_3$Im), or piperidine. These ferryl

$$2PFe^{II} + O_2 \rightarrow PFe^{III}\text{-}O\text{-}O\text{-}Fe^{III}P \qquad (I)$$

$$2B + PFe^{III}\text{-}O\text{-}O\text{-}Fe^{III}P \rightarrow 2BPFe^{IV}O \qquad (II)$$

complexes, $BPFe^{IV}O$, are unstable intermediates which have been detected spectroscopically in solution over the temperature range -90 to -30 °C. Magnetic susceptibility and ^1H NMR spectral studies indicate that they have a well-defined triplet ground state. Warming solutions of $BPFe^{IV}O$ to room temperature results in the disappearance of this intermediate due to its decomposition to form the well-known $PFe^{III}\text{-}O\text{-}Fe^{III}P$.

The characterization of these important ferryl intermediates requires the full identification of all ligands present. In this context, the ligand trans to the ferry group has received very limited characterization. The presence of a sixth ligand was inferred from quantitative titration data which demonstrated the uptake of 1 mol of amine per iron in reaction 2.[6] In this article we report the direct detection of the axial ligands and interface these observations with studies on intact proteins. Because of the

inherent low intensity of these resonances and their large line widths, it was not possible to detect them in our earlier studies conducted on a 100-MHz instrument.[1,6]

Ferryl complexes have been implicated in the reaction mechanisms of peroxidases and cytochromes P-450. For horseradish peroxidase, two intermediates are spectroscopically detectable.[7] Compound I, which is formed upon addition of peroxide to the resting (Fe(III)) form of the enzyme, is widely believed to consist of an $(Fe^{IV}O)^{2+}$ unit complexed by a porphyrin π radical. Compound II, which is obtained upon one-electron reduction of compound I, also possesses a $(Fe^{IV}O)^{2+}$ unit complexed by a normal porphyrin dianion. A related species, ferryl myoglobin, is prepared by the addition of peroxide to myoglobin.[8] It has physical characteristics closely similar to those of compound II of horseradish peroxidase. For cytochrome P-450, the generation of the active oxidizing form of the enzyme is the least well-understood process in the enzymatic cycle, but there is considerable speculation about the presence of a $(Fe^{IV}O)^{2+}$ unit bound to a porphyrin radical as the active oxidant.[9]

In order to establish the identity of the reactive species in proteins, it is useful to compare a wide array of physical properties of clearly identified model compounds with those of the protein. Electronic spectra,[1] magnetic susceptibility,[1] ^1H NMR hyperfine shifts,[3] Mössbauer spectra,[10] and X-ray absorption edge and fine structure spectroscopy[11] have already indicated that synthetic $BPFe^{IV}O$ obtained from (1) and (2) and HRP-II are extremely

(1) Chin, D. H.; Balch, A. L.; La Mar, G. N. *J. Am. Chem. Soc.* **1980**, *102*, 1446.

(2) Chin, D. H.; La Mar, G. N.; Balch, A. L. *J. Am. Chem. Soc.* **1980**, *102*, 5945.

(3) Chin, D. H.; La Mar, G. N.; Balch, A. L. *J. Am. Chem. Soc.* **1980**, *102*, 4344.

(4) La Mar, G. N.; de Ropp, J. S.; Latos-Grazynski, L.; Balch, A. L.; Johnson, R. B.; Smith, K. M.; Parish, D. W.; Cheng, R.-J. *J. Am. Chem. Soc.* **1983**, *105*, 782.

(5) Latos-Grazynski, L.; Balch, A. L.; La Mar, G. N. "Electrochemical and Spectroscopic Studies of Biological Redox Components"; Kadish, K. M., Ed.; Wiley: New York, 1982; *Adv. Chem. Ser.* No. 201, 661.

(6) Chin, D. H. Ph.D. Thesis, University of California, Davis, 1979.

(7) Dunford, H. B.; Stillman, J. S. *Coord. Chem. Rev.* **1976**, *19*, 187.

(8) King, N. K.; Winfield, M. E. *J. Biol. Chem.* **1963**, *238*, 1520.

(9) Groves, J. T. In "Inorganic Biochemistry"; Eichhorn, G. L., Marzilli, L. G., Eds.; Elsevier: New York, 1979; p 119.

(10) Simonneaux, G.; Scholz, W. F.; Reed, C. A.; Lang, G. *Biochim. Biophys. Acta* **1982**, *716*, 1.

(11) Penner-Hahn, J. E.; McMurry, T. J.; Renner, M. W.; Latos-Grazynski, L.; Eble, K. S.; Davis, I. M.; Balch, A. L.; Groves, J. T.; Dawson, J. H.; Hodgson, K. O. *J. Biol. Chem.* **1983**, *258*, 12761.

Table I. Nuclear Magnetic Resonance Parameters for (Base) (Tetra-*m*-tolylporphyrin)Fe^{IV}O

| base	obsd[a] shift, ppm	line width,[a] Hz	isotropic[b] shift, ppm	dipolar shift, ppm	contact shift, ppm
pyridine					
2,6-H	−27.5	3000	−28.5	−7.4	−21.1
4-H	−5.9	240	−11.5	−3.5	−8.0
4-methylpyridine					
2,6-H	−28.0	2000	−29.0	−7.4	−21.6
4-CH$_3$	1.5	20	−0.9	−2.4	1.5
3,4-dimethylpyridine					
2,6-H	−28.9	2900	−30.0	−7.4	−23.6
3,5-H	−4.3	254	−6.7	−2.5	−4.2
4-H	−6.1	270	−11.7	−3.5	−8.2
3-methylpyridine					
2,6-H	−27.0	2350	−28.0	−7.4	−20.6
5-H	−1.4	250	−6.2	−4.0	−2.2
3-H	−4.5	312	−6.9	−2.5	−4.4
4-H	−5.9	378	−11.5	−3.5	−8.1
1-methylimidazole					
1-CH$_3$	2.7	20	1.1	−2.8	3.9
2-H	−22.5	2000	−23.4	−7.5	−15.9
4-H	−17.5	1700	−17.9	−7.3	−10.6
5-H	−2.8	300	−7.0	−4.7	−2.3
1,2-dimethylimidazole					
1-CH$_3$	2.7	20	1.1	−2.8	3.9
4-H	−13.7	2200	−13.0	−7.3	−5.7
5-H	−1.7	300	−5.9	−4.7	−1.2
1,4-dimethylimidazole					
1-CH$_3$	2.7	15	1.1	−2.8	3.9
2-H	−20.5	2300	−21.3	−7.5	−13.8
5-H	−3.1	400	−7.3	−4.7	−2.6
1,5-dimethylimidazole					
1-CH$_3$	2.7	10	1.1	−2.8	3.9
2-H	−23.5	2000	−24.3	−7.5	−16.8
4-H	−15.8	2000	−16.2	−7.3	−8.9
5-CH$_3$	−1.3	70	−1.6	−2.7	1.1

[a] At −50 °C in toluene-d_8. [b] Reference is the analogous diamagnetic ruthenium(II) porphyrin (ref 19).

similar. X-ray absorption fine structure studies have estimated the Fe–O bond length to be short, 1.6 Å. For paramagnetic complexes, the ^{1}H NMR hyperfine shift patterns, which have been shown to be extremely sensitive indicators of the electronic structure of iron,[5] are uniquely useful. The only set of resolved heme resonances, the meso H's, have already been shown to be consistent with the presence of Fe^{IV}O in both HRP-II and ferryl myoglobin.

A further test of the iron electronic structure particularly relevant to the state of axial ligation is the pattern of the hyperfine shifts of the coordinated histidyl imidazole. Herein we show that the hyperfine shift pattern of these axial ligand resonances in BPFe^{IV}O is indicative of the presence of a strong oxo ligand, and we locate two of the axial histidyl peaks in ferryl mobglobin. These observations further support the presence of an unprotonated Fe^{IV}O unit at the active site.

Results

The ferryl complexes were obtained via (1) and (2). Dioxygen was added to a cold (−80 °C) toluene-d_8 solution of (tetra-*m*-tolylporphyrin)iron(II), TmTPFe[11]. The appropriate amine was then added to this cold solution, and the ^{1}H NMR spectrum was recorded. TmTPFe[11] was employed because of its relatively good solubility which produced concentrations that allowed observations of the broad resonances of the axial bases. The numbering schemes used to denote substitution on the coordinated pyridine or imidazole are shown in **1** and **2** below. Identification of resonances
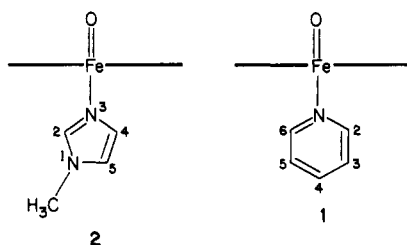
due to the axial amine and the porphyrin in these ferryl complexes was established in each and every case reported below by taking advantage of the thermal instability of BPFe^{IV}O.[1,4] The spectrum of the intermediate prepared at low temperature was obtained at −50 °C. The sample was warmed to room temperature and then cooled to −50 °C. Only those paramagnetically shifted resonances which disappeared in the process were assigned to the variously substituted forms of BPFE^{IV}O.

Assignments for Pyridine Complexes. Because of its greater symmetry, pyridine coordination will be considered first. The 360-MHz ^{1}H NMR spectrum of (pyridine)TmTPFe^{IV}O is shown in trace I of Figure 1. The pyrrole and *m*-tolyl resonances were identified by selective deuteration in previous work.[1] These were used as intensity standards in assigning other resonances. Two upfield resonances at −6 and −28 ppm are assigned to the axially coordinated pyridine. The spectrum of (4-methylpyridine)-TmTPFe^{IV}O shown in trace II lacks the resonance at −6 ppm in trace I. This allows the H-4 resonance to be assigned to the feature at −6 ppm. The spectra of (3-methylpyridine)TmTPFe^{IV}O and (3,5-dimethylpyridine)TmTPFe^{IV}O in traces III and IV of Figure 1 show methyl resonances at −5 ppm and also show the very broad resonance at −28 ppm. As a result, this very broad resonance is assigned to the 2,6 protons. The 3 and 5 protons reside under the solvent resonances between 0 and 3 ppm. In the case of the 3-methylpyridine complex, the H-5 resonance occurs at sufficiently high field so that it is shifted out from under the solvent envelope. In order to confirm the assignment of the 3 and 5 protons, the ^{2}H NMR spectrum of (pyridine-d_5)TmTPFe^{IV}O was examined. Three paramagnetically shifted resonances for the intermediate were observed at 1.5, −5.4, and −28.7 ppm. The resonance at 1.5 ppm is assigned to the 3 and 5 protons.

The chemical shift and proton line-width data for these complexes are collected in Table I. The greater line widths for the 2 and 6 protons as compared to the 4 protons are in good agreement with predictions made on the basis of an r^{-6} dependence that results from the dipolar relation contribution dominating the line width.[12]
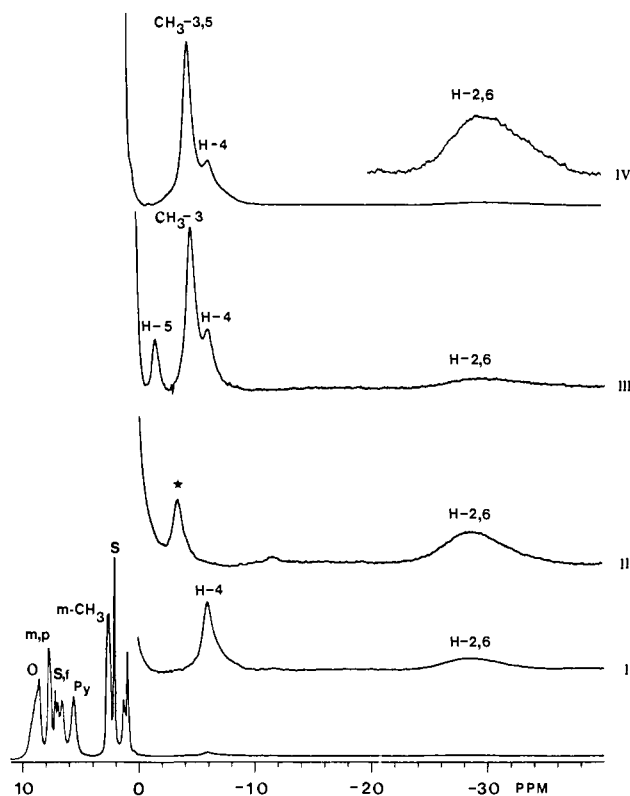

2

1

Axial Amine Coordination

J. Am. Chem. Soc., Vol. 107, No. 11, 1985 3005

Figure 1. 360-MHz ^{1}H NMR spectra of (I) (py)TmTPFe^{IV}O, (II) (4-methylpyridine)TmTPFe^{IV}O, (III) (3-methylpyridine)TmTPFe^{IV}O, and (IV) (3,5-dimethylpyridine)TmTPFe^{IV}O in toluene-d_8 at −50 °C. The assignments for the resonances are as follows: o, ortho phenyl protons; m, p, meta and para phenyl protons; py, pyrrole protons; m-CH$_3$, meta methyl phenyl protons; f, uncoordinated pyridine; s, residual solvent peaks; *, impurity peaks of low spin [B$_2$PFe^{III}]$^+$ complex; H-4, H-5, H-2,6, CH$_3$-3, and CH$_3$-3,5 as the coordinated pyridine protons.

The intensity of the pyridine resonances relative to the pyrrole resonance in these complexes indicates that only one pyridine is bound. Individual resonances can be detected for free and coordinated pyridine; consequently, ligand exchange is slow on the NMR time scale ($\ll 10^4$ s^{-1}).

Resonance Assignments for Imidazole Complexes. Trace I of Figure 2 shows the 360-MHz ^{1}H NMR spectrum of (1-CH$_3$Im)TmTPFe^{IV}O. As with (pyridine)TmTPFe^{IV}O, the pyrrole and m-tolyl resonances were identified from previous work.[1] The identity of the individual resonances of coordinated 1-CH$_3$Im has been determined by their relative intensity and by methyl and deuterium labeling. The three upfield resonances at −3, −17, and −22 ppm each have the intensity of one proton relative to the pyrrole resonance and are due to the ring imidazole protons. The resonance at 2.5 ppm has intensity corresponding to three protons and is assigned to the 1-methyl group. The spectrum of TmTP-Fe^{IV}O (1,2-dimethylimidazole) shown in trace II of Figure 2 lacks the H-2 resonance while the spectrum of (1,4-dimethyl-imidazole)TmTPFe^{IV}O in trace III lacks the H-4 resonance. In both cases, we have been unable to detect resonances of the new methyl groups, and we presume that they are hidden in the crowded region between 0 and 10 ppm. These resonances are also expected to be very broad (vide infra) and consequently difficult to observe. In traces II and III, the H-4 and H-2 resonances occur at lower field than seen in trace I. This probably results from some degree of bending of the coordinated imidazoles. Such bending is caused by the positioning of the 2- or 4-methyl groups near the porphyrin plane. For (1,5-dimethylimidazole)-TmTPFe^{IV}O, the H-5 resonance is absent, but the CH$_3$-5 resonance is readily detected at −1 ppm.
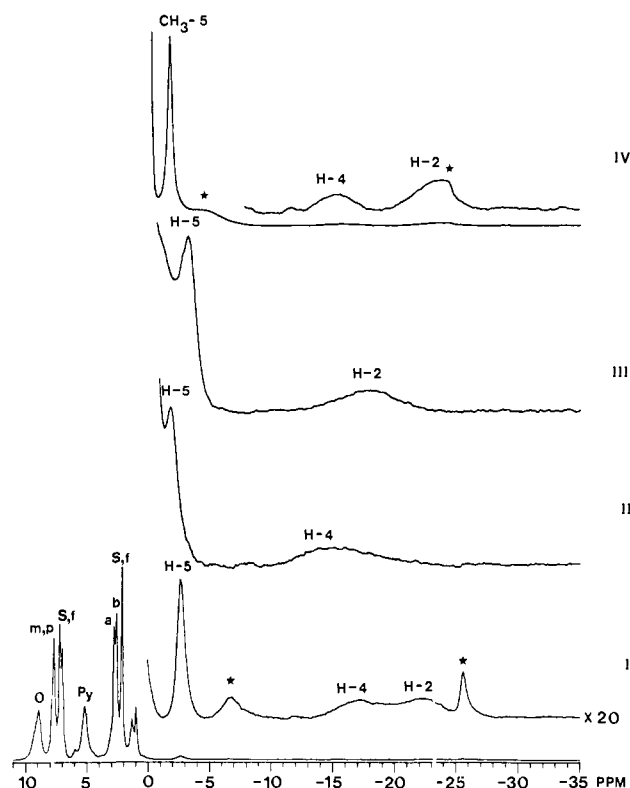
(12) Swift, T. J. In "NMR of Paramagnetic Molecules"; La Mar, G. N., Horrocks, W. D., Holm, R. H., Eds.; Academic Press: New York, 1973; p 53.

Figure 2. 360-MHz ^{1}H NMR spectra of (I) (1-CH$_3$Im)TmTPFe^{IV}O, (II) (1,2-dimethylimidazole)TmTPFe^{IV}O, (III) (1,4-dimethyl-imidazole)TmTPFe^{IV}O, and (IV) (1,5-dimethylimidazole)TmTPFe^{IV}O in toluene-d_8 at −50 °C. Assignments for the various resonance follow Figure 1; H-2, H-4, H-5, and CH$_3$-5 are the coordinated imidazole protons; f, uncoordinated imidazole; a, 1-methyl of coordinated imidazole; b, meta methyl phenyl protons.
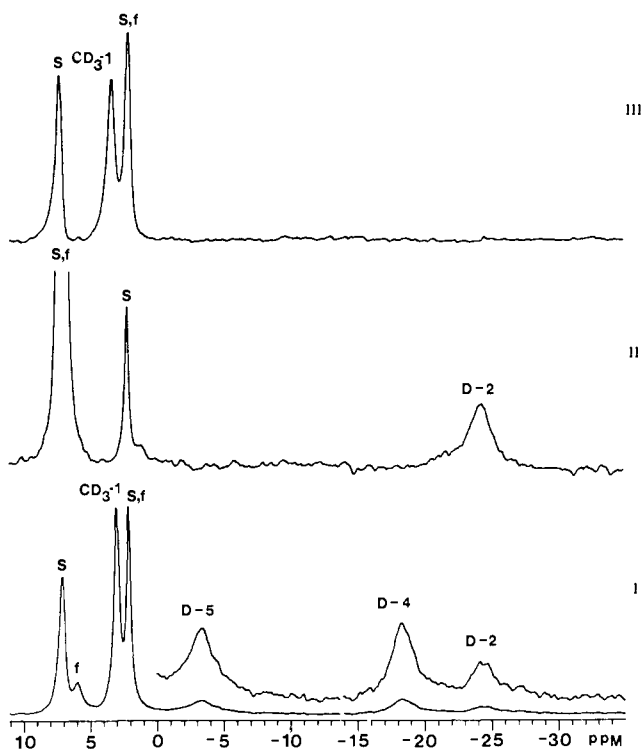

Figure 3. 55.27-MHz ^{2}H NMR spectra of (I) (1-CD$_3$Im-d_3)-TmTPFe^{IV}O, (II) (1-CH$_3$Im-2-d)TmTPFe^{IV}O, and (III) (1-CD$_3$Im)-TmTPFe^{IV}O in toluene at −50 °C. Assignments of the resonance are indicated according to the scheme used in Figure 1. The D-2 resonance is less intense in I from loss of ^{2}H due to chemical exchange.

Since the H-4 and H-2 assignments are not unambiguous from the data in Figure 2 due to the shifts in resonance positions caused

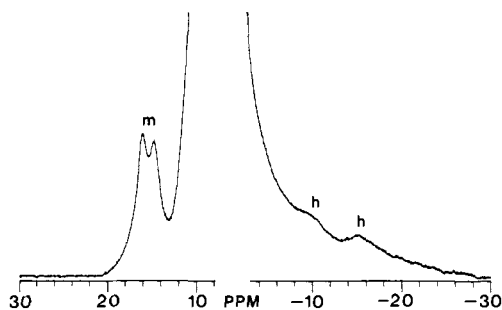**Figure 4.** 360-MHz ^{1}H NMR spectrum of ferryl myoglobin in 0.2 M NaCl 99.8% ^{2}H$_2$O at pH 7.8, 35 °C. The meso porphyrin resonances are denoted by m and the histidine resonances by h. The diamagnetic envelope has been cut off.

by steric factors introduced upon methyl substitution, the assignments were verified by specific deuterium labeling. Trace I of Figure 3 shows the ^{2}H NMR spectrum of (1-MeIm-d_6)-TmTPFe^{IV}O. The four resonances of the coordinated ligand (as well as resonances from the free ligand and natural abundance deuterium in the toluene) are seen at positions corresponding to the resonances assigned to the ^{1}H NMR spectrum. The intensity of the D-2 resonance is lower than that of the D-4 and D-5 resonances because our sample of 1-MeIm-d_6 was incompletely deuterated at the 2-position due to the readily exchangeable nature of the substituent at that site. Trace II, which shows the spectrum of (1-methylimidazole-2-d)TmTPFe^{IV}O, allows the unambiguous identification of the D-2 resonance. Trace III of Figure 3 shows the spectrum of (1-methyl-d_3-imidazole)TmTPFe^{IV}O.

The resonance positions and ^{1}H line widths are collected in Table I. The proton line widths, which increase in the order 1-CH$_3$ < 5-CH$_3$ < 5-H < 4-H ~ 2-H, are in reasonable agreement with predictions made on the basis of an inverse sixth power of the iron-proton distance, r^{-6}.[13] Such predictions indicate that the 2-methyl and 4-methyl resonances should be 1500–2300 Hz wide. Consequently if they occur, as we suspect, in the crowded region 0–10 ppm, they will be too broad for detection.

Since separate resonances have been observed for free and coordinated imidazole (see trace I of Figure 3 particularly), axial ligand exchange in slow ($\ll$3 × 10^3 s^{-1}).

Axial Histidine Resonances in Ferryl Myoglobin. The preceding results on model compounds suggest that the proximal histidyl imidazole ligands in ferryl myoglobin and in compound II of horseradish peroxidase should produce broad resonances in the upfield region. Previous ^{1}H NMR spectra of these protein intermediates focused on well-resolved and relatively narrow resonances and did not possess sufficient signal-to-noise to allow identification of very broad resonances. A ^{1}H NMR spectrum of ferry myoglobin obtained under conditions that would facilitate the observation of the broad upfield resonances is illustrated in Figure 4. In addition to the downfield-shifted meso resonances at 17 ppm, two broad resonances of low intensity are observed at ca. −11 and −16 ppm. These are assigned to the proximal histidyl imidazole 2-H, 4-H. The occurrence of these resonances accompanies the presence of the meso resonances at ca. 17 ppm, and there is no question that they belong to a single intermediate of limited stability. The assignment of these upfield resonances to 2-H and 4-H of an axial hystidyl residue is supported by line-width considerations. Dipolar relaxation (αr^{-6}) predicts 2-H and 4-H line widths to be 5 to 7 times larger than the meso-H line widths. The 350–400-Hz line width for the meso H and the ~2-KHz line width for the upfield resonances are clearly consistent with expectation. Primarily because of the lower stability associated with compound II of horseradish peroxidase, we have not been able to detect similar upfield resonances for this intermediate.

Discussion

Magnetic Anisotropy of Ferryl Heme. The use of hyperfine shifts to elucidate magnetic and electronic properties of para-
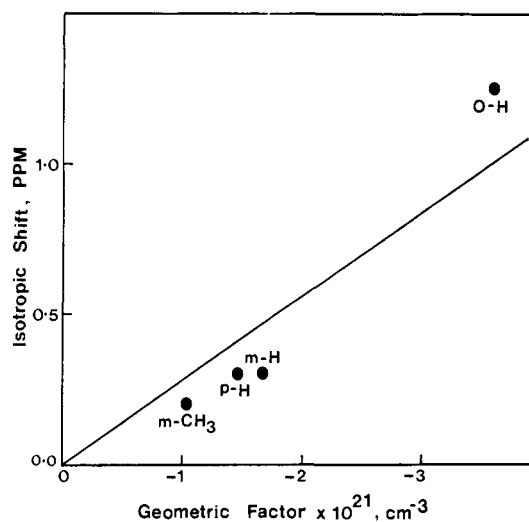
Figure 5. Plot of the isotropic shifts for (1-CH$_3$Im)TmTPFe^{IV}O at −50 °C vs. the calculated geometric factor $(3 \cos^2 \theta - 1)r^{-3}$.

magnetic metalloporphyrins first requires the knowledge of the relative magnitudes of the contact and dipolar contribution to the hyperfine shifts, eq 1.[14] The dipolar shift in axial symmetry is

$$(\Delta H/H)^{hf} = (\Delta H/H)^{con} + (\Delta H/H)^{dip} \qquad (1)$$

given by the familiar relationship eq 2 where $\chi_\parallel$ and $\chi_\perp$ are

$$(\Delta H/H)^{dip} = \frac{1}{3} (\chi_\parallel - \chi_\perp)(3 \cos^2 \theta - 1)r^{-3} \qquad (2)$$

components of the axial susceptibility tensor, θ is the angle between the iron-proton vector and the symmetry axis, and r is the length of the vector.[14] While the magnetic anisotropy is not known, it has been demonstrated that NMR can directly yield quantitative estimates from the hyperfine shifts under favorable circumstances if the dipolar shift can be experimentally determined.[15]

Thus, a variety of low-spin tetraarylporphyrin complexes have been shown to exhibit hyperfine shifts for the meso-aryl substituent that are wholly dipolar in nature because of insulation of this group from transferred spin density.[14] This dominance of $(\Delta H/H)^{dip}$ for the meso-aryl group can be established by the linearity of a plot of $(\Delta H/H)^{hf}$ on the calculated geometric factor $(3 \cos^2 \theta - 1)r^{-3}$ for nonequivalent protons. Such a plot is illustrated in Figure 5 for (1-CH$_3$Im)TmTPFe^{IV}=O and confirms the dominance of the dipolar interaction. The strict Curie behavior for all hyperfine shifts has been reported previously.[1] Using the ~1 ppm dipolar shift for o-H and the known geometric factor, we determine at −80 °C

$$\Delta \chi = \chi_\parallel - \chi_\perp = -250 \times 10^{-6} \text{ cgs}$$

This anisotropy together with the bulk susceptibility, $\chi = \frac{1}{3}(\chi_\parallel + 2\chi_\perp) = 5450 \times 10^{-6}$ cgs, yields $\chi_\parallel = 5283 \times 10^{-6}$ and $\chi_\perp = 5533 \times 10^{-6}$ cgs. This translates to $\mu_\parallel = 2.87$, $\mu_\perp = 2.93$ μ_B for the $S = 1$ system. The nearly identical porphyrin shifts for pyridine and 1-methylimidazole as axial ligands indicate that the electronic structure is the same for both axial ligands.

The susceptibility data indicate a low-spin $S = 1$ state. A very substantial tetragonal distortion is required to quench the orbital contribution to the presumed $^3T(O_h) \rightarrow {}^2A(C_{4v})$ ground state and result in such small magnetic anisotropy. These findings are consistent with experimental MO calculations[16-18] for BPFe^{IV}O

(13) Satterlee, J. D.; La Mar, G. N. *J. Am. Chem. Soc.* **1976**, *98*, 2804.

(14) La Mar, G. N.; Walker, F. A. In "The Porphyrins"; Dolphin, D., Ed.; Academic Press: New York, 1979; Vol. 4, pp 61–157.

(15) Goff, H.; La Mar, G. N.; Reed, C. A. *J. Am. Chem. Soc.* **1977**, *99*, 3641.

(16) Loew, G. H.; Kert, C. J.; Hjelmeland, L. M.; Kirchner, R. F. *J. Am. Chem. Soc.* **1977**, *99*, 3534.

(17) Loew, G. H.; Herman, Z. S. *J. Am. Chem. Soc.* **1980**, *102*, 6173.

(18) Hanson, L. K.; Chang, C. K.; Davis, M. S.; Fajer, J. *J. Am. Chem. Soc.* **1981**, *103*, 663.

which reveal a very strong destabilization (1 eV) of the π-antibonding (and spin containing) d_{xz}, d_{yz} orbitals relative to the nonbonding d_{xy} iron orbitals.

Iron–Axial Ligand Bonding. The knowledge of the o–H (H_i) shifts and the relative geometric factors allows the determination of the dipolar contribution for any H_j via eq 3.[14] The resulting

$$(\Delta H/H)_j^{\text{dip}} = (\Delta H/H)_i^{\text{dip}}(3\cos^2\theta_j - 1)r_j^{-3}/(3\cos^2\theta_i - 1)r_i^{-3} \tag{3}$$

$(\Delta H/H)_j^{\text{dip}}$ are listed in Table I. These together with the observed $(\Delta H/H)_j^{\text{hf}}$ (referenced against the analogous diamagnetic Ru(II) complexes)[19] yield the contact shifts (given in the last column of the Table I) for both the porphyrin pyrrole-H and the axial ligands.

For axial imidazoles, the resulting contact shifts exhibit a pattern very similar to that observed earlier for low-spin ($S = 1/2$) ferric bis(imidazolate) and monoimidazolate, monocyano complexes which have been shown to be consistent with imidazole $\rightarrow$ iron π donation involving the highest filled imidazole π MO.[13,20] While the relative magnitudes and signs of the nonequivalent imidazole proton contact shifts are similar, however, the magnitudes are generally smaller by a factor of 2 for the ferryl than the ferric low spin species. When considering the fact that the ground state for low-spin iron(IV) has two and low-spin iron(III) has only one π-bonding unpaired electron, the axial imidazole π covalency in the ferry complex (λ^2 in the antibonding orbital $\psi_A = N(d_{xz} - \lambda\phi)$) is only 20% of that in low-spin ferric complexes.[21] This is consistent with the fact that such covalency will be reduced as the d orbital energies are lowered by oxidation of the metal center and that the trans oxo ligand in the ferryl species is a much stronger ligand than the imidazole.

In the case of axial pyridines, the dominant π bonding leads to spin polarization effects by the d_π spin, again leading to contact shift patterns very similar to those reported for the axial base in low-spin ferric bis(pyridine), except that the shifts are again smaller in the ferryl species.

Thus, both the small axial ligand shifts as well as small porphyrin pyrrole-H shifts dictate that the unpaired spin must be localized primarily on the $Fe^{IV}O$ unit in a MO involving the iron d_{xz}, d_{yz} and the oxygen, p_x, p_y orbitals. Such a highly localized ground state has also been predicted on the basis of MO calculations.[16–18] Moreover, the MO results predict that the unpaired spins are even more localized in the $Fe^{IV}O$ fragment in the unligated ferryl species $PFe^{IV}O$ than in the ligated complex (B)$PFe^{IV}O$. In accordance with this, our ^1H NMR data have shown that the pyrrole-H shift is even smaller in the former complex.[23]

Since very sizable contact shifts have been reported[24] for other d^4 metalloporphyrins which possess the same type of unpaired metal spins for delocalization except that the axial ligands are weaker donors than the oxo ligand, we propose that the small contact shifts in ferryl complexes, particularly for the currently characterized axial ligands, are significant indicators of the strong oxo π bonding.

Axial Ligation in Ferryl Myoglobin. The essentially identical and highly characteristic meso-H hyperfine shifts in the model $BPFe^{IV}O$ and in ferryl myoglobin as well as in HRP-II confirm very similar iron–porphyrin bonding for a low-spin iron(IV) state. However, since HRP-II conversion to HRP-I involves the loss of both an electron (from the porphyrin) and a proton,[25] it has generally been assumed that one species possesses an oxo and the other a hydroxyl ligand. The suggestion based on ENDOR that

a proton is absent HRP-I indicates the need for additional data on the axial ligand in HRP-II (and its isoelectronic analogue, ferryl myoglobin).

The appearance of two broad peaks with single proton intensity in the upfield region where the axial imidazole 2-H and 4-H signals resonate in the model complexes allows for reasonable assignment to the same functional groups. This confirms that the iron–histidyl imidazole bonding in ferryl myoglobin (and hence by inference for HRP-II) is again unique and essentially the same as in (1-CH_3Im)$TmTPFe^{IV}O$. Again, this small degree of axial imidazole spin delocalization must be interpreted in terms of a very strong donor ligand such as the oxo species and is inconsistent with the presence of the much weaker hydroxy ligand. Thus, we conclude that the presently characterized axial imidazole hyperfine shift data, together with our earlier assignments of heme resonances, are strongly indicative of an active site in ferryl Mb and HRP-II which contains an oxo-ligated low-spin iron(IV) porphyrin bond to the proximal histidyl imidazole.

Experimental Section

Materials. $TmTPFe^{III}Cl$,[26,27] 1-methylimidazole-d_6,[28] 1-methyl-d_3-imidazole,[28] 1-methylimidazole-2-d,[29] 1,4-dimethylimidazole,[30] and 1,5-dimethylimidazole[30] were obtained by previously established routes. Substituted pyridines (Eastman) and 1,2-dimethylimidazole (Aldrich) were obtained commercially. The pyridines were distilled and stored over activated molecular sieves before use. Toluene-d_8 (Aldrich) and AR-grade toluene (Mallinkrodt) were deoxygenated by three freeze–pump–thaw cycles and stored over activated molecular sieves under argon in a Vacuum Atmosphere glovebox.

Preparation of (Base)$TmTPFe^{IV}O$. The $TmTPFe^{II}$ was prepared by the reaction of $TmTPFe^{III}Cl$ in toluene by using zinc–amalgam[23] in a Vacuum Atmosphere glovebox under argon. The solution was filtered to remove the amalgam and zinc chloride. A $\sim$2 mM solution of PFe^{II} was placed into an NMR tube and sealed with a septum cap. The sample was removed from the controlled-atmosphere box and cooled to -80 °C. Dioxygen was introduced into the sample through a syringe needle. $TmTPFe$-O-O-$FeTmTP$ formed after the cold solution was gently shaken. A toluene solution of the appropriate base was then added to the sample through a microsyringe while the sample was maintained at -70 °C. A 2–3 M excess of base per iron was present.

Ferryl Myoglobin. The protein sample was prepared from a fourfold excess of hydrogen peroxide to ferric myoglobin as described previously.[4,8]

NMR Measurements. NMR spectra were obtained on a Nicolet NT-360 FT NMR spectrometer operating in the quadrature mode (^1H frequency, 360 MHz). Between 500 and 20 000 transients were accumulated over 4-40-KHz bandwidth with 4–8K data points and a 6-μs 90° pulse. The proton spectra were accumulated by using a SPLAPO pulse sequence to suppress the methyl signal of toluene with a 1-s low-power pulse at 18 dB and decoupling the phenyl signals of toluene. Signal-to-noise ratio was improved by apodization of the free induction decay which introduced a negligible 15–30-Hz line broadening. The residual methyl peak of toluene was used as a secondary reference, this being set at 2.09 ppm. In order to obtain integrated areas of the various resonances, the spectra were deconvoluted by using the NTCCAP routine of the Nicolet Software.

(19) Faller, J. W.; Chen, C. C.; Malerich, C. J. *J. Inorg. Biochem.* **1979**, *11*, 151.

(20) Chacko, V. P.; La Mar, G. N. *J. Am. Chem. Soc.* **1982**, *104*, 7002.

(21) La Mar, G. N. *Inorg. Chem.* **1971**, *10*, 2633.

(22) La Mar, G. N.; Bold, T. J.; Satterlee, J. D. *Biochim. Biophys. Acta* **1977**, *498*, 189.

(23) Balch, A. L.; Chan, Y.-W.; Cheng, R.-J.; La Mar, G. N.; Latos-Grazynski, L.; Renner, M. W. *J. Am. Chem. Soc.* **1984**, *106*, 7779.

(24) Hansen, A. P.; Goff, H. M. *Inorg. Chem.* **1984**, *23*, 4519.

(25) Yamazaki, I.; Araiso, T.; Hayashi, Y.; Yamada, H.; Makino, R. *Adv. Biophys.* **1978**, *11*, 249.

(26) Alder, A. D.; Longo, F. R.; Finarelli, J. D.; Goldmacher, J.; Assour, J.; Korsakoff, L. *J. Org. Chem.* **1967**, *32*, 476.

(27) Alder, A. D.; Longo, F. R.; Kempas, F.; Kim, J. *J. Inorg. Nucl. Chem.* **1979**, *32*, 2443.

(28) Hodges, R.; Grimmett, M. R. *Aust. J. Chem.* **1968**, *21*, 1085.

(29) Vaughan, J. D.; Mughrabi, Z.; Wu, E. C. *J. Org. Chem.* **1970**, *35*, 1141.

(30) Takeuchi, Y.; Yeh, H. J. C.; Kirk, K. L.; Cohen, L. A. *J. Org. Chem.* **1978**, *43*, 3565.